High Molecular Weight Poly(aromatic amide) Foldamers via Living Polymerization

Subhajit Pal, Linda Hong, Rafael V.M. Freire, Saquib Farooq, Stefan Salentinig and Andreas F. M. Kilbinger*

Department of chemistry, University of Fribourg, Chemin du Musée 9, 1700 Fribourg, Switzerland.

KEYWORDS: living polycondensation, aramids, foldamers, helices

ABSTRACT: Polyaromatic amides (aramids) have been an important class of industrial polymers and have recently been extensively studied for biomimetic foldamer design. The inherent rigid structure and strong H-bonding make linear aramids notoriously insoluble in non-H-bond breaking solvents and they are typically synthesized via polycondensation in H-bond breaking solvents. Here we report a chlorophosphonium iodide reagent that can activate aromatic carboxylic acids in the presence of aromatic primary and secondary amines. The synthesized reagent is inert towards H-bond-breaking solvents like DMAc and NMP and allows living polymerization of aromatic amino acid monomers and oligomers in H-bond-breaking solvents for the first time. A foldamer forming monomer was also polymerized in a living chain-growth fashion. AFM, SEM, SAXS, and CD spectroscopy analyses strongly supported the tubular helical nature of the synthesized foldamer.

INTRODUCTION

Linear aromatic polyamides (aramids) have attracted significant attention over the past decades. The inherent chain extended structure arises from the partial double bond character of the amide bond. The presence of hydrogen bonding and aromatic-aromatic interactions further provide high mechanical strength, thermal stability, and shape persistence.[1,2,3,4] Due to these features, such aramids are only soluble in H-bond accepting solvents like DMAc, NMP, DMF, and concentrated sulfuric acid.[2,4] Since the discovery of poly(p-phenylene terephthalamide) (Kevlar) by Kwolek at DuPont, aramids have become an industrially important class of polymers.[5] Nevertheless, aramids also attracted significant attention from organic and biochemists due to their shape-persistent nature.[6,7,8,9,10] The rigid conformation and the ability to form ordered solution structures make aramids excellent candidates for complex supramolecular architecture design and this has recently been studied by our group and others.[11,12,13,14,15,16,17,18,19]

Recently, a growing interest has been in developing polymers (foldamers) that can adopt a well-defined 3-dimensional structure in solution and eventually mimic protein-like functions. In this context, aromatic amide foldamers are amongst the most studied ones.[20,21,22,23,24,25,26,27] The groups of Huc, Gong, our own, and others have designed a library of foldamers based on aromatic amides that fold into a helical shape with tunable cavity size.[6,9,28,29,30,31,32,33] Recent studies have also shown that the foldamers obtained from aromatic amides can mimic biological functions like transport and recognition.[34,35,36,37,38,39,40]

Although the aromatic amide block copolymers and foldamers show huge potential for materials and biological applications, synthesizing such polymers is challenging. The lack of compatible polymerization conditions limits the synthesis of narrow dispersed high molecular weight foldamers and aramid block copolymers. Moreover, the poor solubility and lower reactivity of the monomers make the convergent synthesis of foldamers extremely difficult.

Polyaromatic amides are mainly synthesized by the polycondensation of amines with carboxylic acids under harsh conditions.[41,42] A typical polycondensation reaction follows step-growth kinetics where monomer, oligomer, and polymer chain-ends can react with each other, and a high extent of conversion is required to achieve high molecular weight polymers with dispersities approaching a value of 2.[43] Additionally, control over molecular weight is often very difficult under step-growth conditions, and syntheses of block copolymers is not feasible out of principle.

As Yokozawa and our group showed, polyaromatic amides can be synthesized with narrow dispersity and good molecular weight control under living chain-growth polycondensation conditions.[44,45,46,47] In 2000, the Yokozawa group developed an innovative approach that involves the self-deactivation of *N*-alkylated AB-type condensation monomers.[48] *N*-alkylated para and meta poly(benzamide)s are the best-investigated polymers in this context.[49,50] In the presence of a strong and bulky base, an *N*-alkylated aminobenzoic ester undergoes deprotonation and forms an amide anion which acts as a strong electron-donating group and deactivates the corresponding ester. This prevents self-condensation and allows a selective reaction with an initiator and later with the growing polymer chain end mimicking chain-growth polymerization kinetics. Although Yokozawa's method shows huge potential for the synthesis of narrowly dispersed homo and block copolymers, the use of a strong base, low temperatures, and some undesired side reactions limit the technique to a lower degree of polymerization (20kDa).[48,51] Simultaneously, the requirement of a highly nucleophilic amide anion restricts electrophilic functionalities and reaction media use. Hence, synthesizing foldamers and complex polymeric architectures becomes challenging under Yokozawa's original conditions. Our group recently reported a versatile living polymerization protocol for mono and oligomeric primary and secondary aromatic amino acids, irrespective of their potential for self-deactivation.[31] We have developed two phosphorous-based reagents, **PHOS1** and **PHOS2** (see Figure 1),

that selectively activate carboxylic acids into acid chlorides in the presence of primary and secondary aromatic amines (see Table 1).

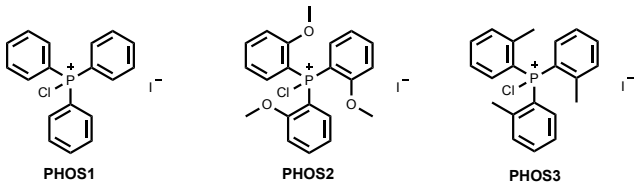

Figure 1. Structures of PHOS reagents.

Table 1. Characteristics of PHOS reagents

Reagent	Acid activation	[a]Amine compatibility	[b]Solvent compatibility
PHOS1	yes	S	cat 1
PHOS2	yes	P, S	cat 1
PHOS3	yes	P, S	cat 1, cat 2

[a] S= aromatic secondary amine, P= aromatic primary amine

[b] cat1 = DCM, $CHCl_3$, DCE, THF, ACN; cat 2 = DMAc, NMP, DMF

In analogy to Yokozawa´s method, the acid chloride acts as an electron-withdrawing group and deactivates the corresponding conjugated amine. This allows the selective propagation from the initiator leading to living chain-growth polymerization. Additionally, fast and efficient carboxylic acid activation also allowed the living chain-growth polymerization of non-self-deactivated monomers and oligomers under slow monomer addition conditions. The slow addition of monomers dramatically reduces the active monomer concentration in the solution, diminishing the unwanted bimolecular self-condensation and allowing pseudo-chain-growth polymerization.[52] This method shows huge potential for synthesizing functional living aramids but finds its limitations at higher temperatures and when H-bond breaking solvents like DMF, DMAc, and NMP are required.

RESULTS and DISCUSSION

Reagent design and compatibility study

The living polymerization of primary aromatic amino acids is immensely challenging due to the formation of strong H-bonding between the secondary amides formed in the polymer. The extended rigid linear structure and strong H-bonding of the secondary amides diminishes the polymer's solubility and hinders the formation of high molecular weights and hence the living homo and block copolymer synthesis. The living polymerization of helical foldamer forming monomers is equally difficult due to their tendency to fold into helices and furthermore aggregate during polymerization. However, the aggregation (stacking) of helical aromatic amide foldamers can be avoided by using polar solvents like DMSO and DMF[53,54] and potentially elevated temperatures.

Scheme 1. General scheme of the living polymerization of non-self-deactivating aromatic amino acids under slow addition conditions (a), the structures of the monomers (b), and the initiators (c) used in this study.

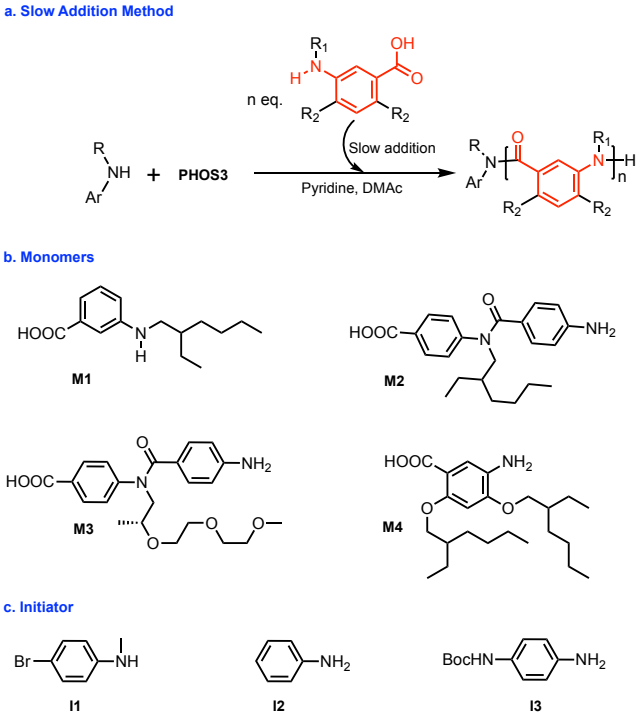

Primary aromatic amine-containing monomers cannot be polymerized in a chain-growth manner under Yokozawa's conditions as the secondary amide formed during polymerization will undergo immediate deprotonation resulting in insolubility and consumption of base. Nonetheless, primary aromatic amino acid monomers and oligomers were polymerized in a living chain-growth manner in our recently reported method. However, the poor solubility of the secondary amide-containing polymer in non-H-bond breaking solvents limits the synthesis to low molecular weights. Similarly, a protected foldamer was synthesized in a two-step process to avoid superstructure formation during polymerization. There, the primary amine was protected as an acid-labile secondary amine to obtain a random coil polymer during synthesis. A post-polymerization deprotection led to the targeted foldamer.[31]

Among the two reagents (**PHOS1** and **PHOS2**, see Figure 1) developed in our group, **PHOS1** is inert towards secondary aromatic amines but reacts irreversibly with primary aromatic amines. **PHOH2**, on the other hand, is inert to both primary and secondary aromatic amines at room temperature but reacts with primary aromatic amines at elevated temperatures. Moreover, both **PHOS1** and **PHOS2** undergo Vilsmeier-Haack-like reactions with solvents like DMF, DMAc, and NMP, and hence, polymerization is inaccessible in such solvents.

To overcome the limitation, we have designed a new reagent, **PHOS3**, which is inert towards primary aromatic amines at elevated

temperatures and compatible with H-bond breaking solvents. We have reported earlier that by lowering the electrophilicity and increasing the steric bulk of the PHOS reagents, a more selective carboxylic acid activation can be achieved. However, a consecutive reduction of electrophilicity and increasing steric bulk can dramatically reduce the carboxylic acid activation rate and lead to the accumulation of inactivated monomers, which could act as an initiator and hamper living polymerization. Hence, we only focused on the increasing steric bulk at the reagent center. By increasing the steric bulk at the catalytic phosphorous site, we can obtain a selective carboxylic acid group activation over the reactions with bulkier aromatic amines and secondary amide group as in H-bond breaking solvents like NMP and DMAc. We hypothesized that we could obtain a more selective reagent by replacing the tri(o-methoxy)phosphine with tri(o-tolyl)phosphine. By placing the methyl group closer to the phosphorus atom we hoped to increase the steric demand of the phosphonium center.

To test the feasibility of our hypothesis, **PHOS3** was synthesized by slow addition of a tri(o-tolyl)phosphine solution (1 M) in chloroform to an ICl solution (1 M) in DCM at 50 °C (see SI, p.7). ^{31}P NMR and HRMS spectroscopy confirmed only one major ionic species present in the solution (δ=63.8 ppm; see SI, p.8). Furthermore, to confirm the active structure of **PHOS3**, and to determine the mechanistic pathway of activation, a model reaction was performed with hexanol and followed by ^{1}H NMR spectroscopy. Astonishingly, alkoxy-attached **PHOS3** was observed in ^{1}H NMR spectroscopy along with the formation of hexyl iodide as the major product (see SI, p.13). This indicates that the substitution reaction takes place via an intermediate pentavalent alkoxy adduct formation where the iodide counter ion is the only nucleophile present in the solution for the nucleophilic substitution. The slower substitution rate may have contributed to the formation of minor hexyl chloride due to the increasing concentration of chloride ions over the reaction.

Next, the potential of carboxylic acid activation of **PHOS3** was investigated by reacting it with benzoic acid and following the reaction by ^{31}P NMR spectroscopy (see SI, p.7). As expected, **PHOS3** cleanly activates the aromatic carboxylic acid in the presence of pyridine as a base (see SI, p.7). Then, another control ^{31}P NMR experiment was performed to determine the inertness of **PHOS3** towards aromatic primary amines at elevated temperatures. Interestingly, when 2eq of **PHOS3** were treated with 1eq of aniline in chloroform-d at 50 °C, no change in ^{31}P spectra was observed even at an extended period (8h), confirming the inertness of **PHOS3** towards aromatic primary amines (see SI, p.8). Subsequently, as the H-bond breaking solvents are of prime interest for aramid synthesis, the DMF, DMAc, and NMP compatibility of **PHOS3** were studied by ^{31}P NMR spectroscopy. In a model ^{31}P NMR reaction, 0.2 mmol of **PHOS3** was dissolved in 1 mL of a chloroform-d and dry DMAc mixture (1:1) and was followed for 13h at rt (see SI, p.9). Interestingly, no significant decomposition of **PHOS3** was observed over the extended course of the reaction, thereby confirming the inertness towards DMAc. In sharp contrast, **PHOS1** and **PHOS2** rapidly decomposed to the corresponding oxide when treated with DMAc under similar conditions (see SI, p.10). Next, the compatibility of **PHOS3** with NMP and DMF was investigated under similar conditions. Interestingly, the excellent compatibility of **PHOS3** towards NMP was confirmed by ^{31}P NMR spectroscopy; however, slow decomposition of **PHOS3** was observed when treated with DMF (see SI, p.12). Due to the significantly smaller size of DMF compared to NMP and DMAc; **PHOS3** reacts with DMF and undergoes decomposition. Nonetheless, the efficient carboxylic acid activation and tolerance towards aromatic primary amines and solvents like DMAc and NMP by **PHOS3** offer a promising scope of living aramid synthesis in H-bond breaking solvents.

Polymerizations of non-self-deactivating monomers

Thereafter, the efficacy of **PHOS3** towards a control polymerization was tested with *N*-alkylated meta-amino benzoic acid under slow addition conditions. We, therefore, added a DMAc solution of 3-((2-ethylhexyl)amino)-benzoic acid (**M1**) via a syringe pump to a solution of initiator 4-bromo-*N*-methylaniline (**I1**) and **PHOS3** in DMAc and chloroform mixture at rt (chloroform was used to enhance the solubility of **PHOS3** in DMAc, see Scheme 1). Excitingly, the SEC analysis of crude polymer shows excellent control over molecular weight with narrow dispersity, whereas ^{1}H NMR spectroscopy analysis confirmed complete monomer consumption immediately after the completion of slow addition (see SI, p.14, p.23). Inspired by the controlled polymerization of secondary aromatic amino acids with **PHOS3**, we next focused on primary aromatic amino acids, as their living polymerization is more challenging. We used a primary amine-containing dimeric amino acid monomer 4-(4-amino-*N*-(2-ethylhexyl)benzamido)benzoic acid (**M2**) due to its non-self-deactivating nature and known helical superstructure of the resulting polymer.[31,55] Therefore, **M2** would allow testing the feasibility of the living polymerization of a superstructure forming and non-self-deactivating monomer with **PHOS3** in DMAc. In the first polymerization, a solution of **M2** in DMAc was added slowly via a syringe pump to a solution of aniline (initiator, **I2**), **PHOS3**, and pyridine (see Scheme 1). After complete monomer addition, the crude polymer mixture was analyzed by SEC and ^{1}H NMR spectroscopy. The number average molecular weight obtained by the SEC (DMF) was a close fit to the targeted monomer-to-initiator ratio (see Table 2). Furthermore, ^{1}H NMR analysis confirmed the complete conversion of the monomer. A perfect linear fit of the number average molecular weight to the monomer to initiator ratio was also found when monomer **M2** was polymerized with different initiator ratios and narrow dispersities, indicating the living nature of the polymerization (see Figure 2A, Table 2). It is worth mentioning that the DP of the polymer synthesized with **PHOS3** in DMAc was twice as high as our previously reported polymerization of **M2** with **PHOS2** in DCM.

Block copolymerizations of chiral monomer

An important feature of living polymerization is its ability to form block copolymers. To confirm the living nature of the polymerization in DMAc with **PHOS3**, two diblock copolymers were synthesized via sequential slow addition of monomers. A chiral dimeric monomer **M3** was considered a first block followed by a racemic second block with monomer **M2**. The first block copolymer (**PB1**) was synthesized by slowly adding 8eq of **M3** followed by 22eq of **M2**, to a solution of **I2**, **PHOS3**, and pyridine. SEC analyses of both first and diblock show a distinct shift of molecular mass distribution, confirming a successful block copolymer formation (see Figure 2C).

Likewise, the second block copolymer (**PB2**) was obtained from sequential polymerization of 15eq **M3** followed by 15eq **M2**, and the block copolymer nature of the copolymer was confirmed by SEC analyses (see Figure 2D). The NMR analyses of both **PB1** and **PB2** also confirmed the block copolymer nature of the copolymer.

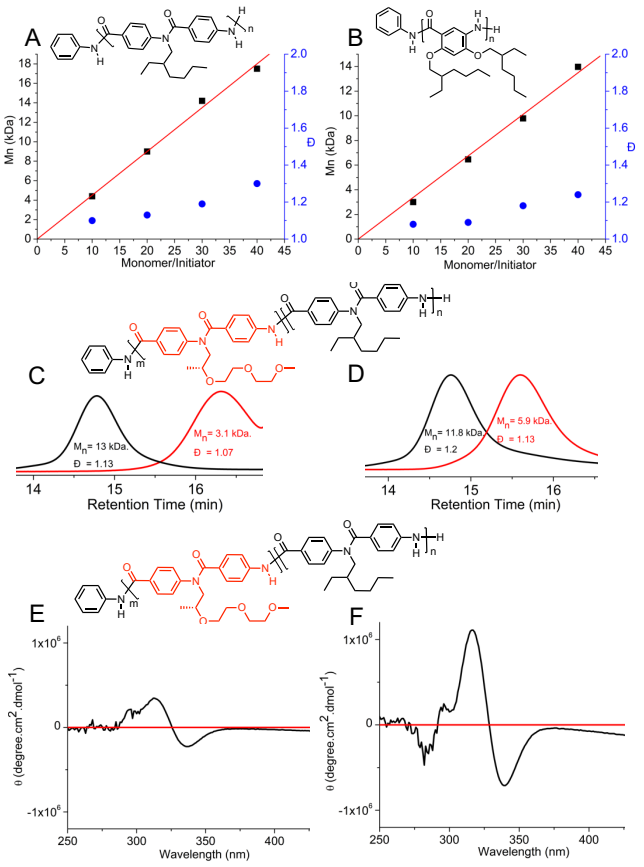

Figure 2. Characteristics of the synthesized polymers. (A and B) Linear plot of the number average molecular weight (SEC) (black squares) versus the monomer: initiator ratio for **M2**:**I2** with **PHOS3** in DMAc(A); **M4**:**I2** with **PHOS3** in chloroform (B). (C and D) Normalized SEC elugram of block copolymer (**PB1** and **PB2**) synthesized from **M3** and **M2** with varying monomer feed ratio **M3**:**M2**= 8:22 (C); M3:M2 = 15:15 (D). CD spectra of the block copolymer (**PB1** and **PB2**) synthesized from **M2** and **M3** with varying monomer feed ratio **M3**:**M2**= 8:22 (E); **M3**:**M2** = 15:15 (F).

Table 2. Number average molecular weights (Mn) and polydispersity indexes (Đ = Mw/Mn) of the polymers synthesized with monomer **M1** and **M2**

Polymer[a]	M/I	M_n-theo [kDa][b]	M_n-SEC [kDa][c]	Đ[c]
P1	16	3.7	3.6	1.1
P2	10	3.5	4.4	1.09
P3	20	7	9	1.13
P4	30	10.5	14.2	1.19
P5	40	14	17.5	1.34

[a] For **P1, M1** and **I1** were employed, **P2**-**P5** were synthesized from **M2** and **I2**.

[b] Theoretical Molecular weight.

[c] Experimental Molecular weight determined by SEC in DMF.

Furthermore, circular dichroism (CD) spectroscopy analysis of both block copolymers confirmed the helical nature of the block copolymer (see Figure 2E, 2F).[55] The higher CD spectra intensity of **PB2** compared to **PB1** also confirmed the targeted higher incorporation of the chiral monomer in **PB2**.

Polymerizations of foldamer forming monomer

Next, the synthesis of an aromatic tubular helix with **PHOS3** was investigated. Therefore, we synthesized the monomer 5-amino-2,4-bis((2-ethylhexyl)oxy)benzoic acid (**M4**) and polymerized it under slow addition conditions at elevated temperatures (55°C) in chloroform (see Scheme 1).[23,26] The higher temperature was considered to avoid aggregation during polymerization, whereas chloroform was chosen as the solvent due to the high solubility of ethylhexyl side chain substituted foldamers. Interestingly, the polymer **P6** obtained from the very first polymerization attempts of **M4** with aniline (**I2**) (10:1) and **PHOS3** shows narrow dispersity and excellent molecular weight control (Table 3). Therefore, a set of polymerizations of M4 was performed with varying initiator (**I2**) ratios (20, 30, and 40:1) at 55°C in chloroform. The obtained polymers (**P7**, **P8**, **P9**) show excellent molecular control with narrow disperities. A perfect linear relationship can be drawn between the monomer to initiator ratio and number-average molecular weights (see Figure 2B, Table 3). This supports the living nature of the polymerization. Furthermore, a clear distinction of proton signals belonging to the end groups and the monomer repeating units in ^{1}H NMR spectroscopy allowed the determination of the number average molecular weight of the purified polymers (see Table 3). Furthermore, an isotopically resolved MALDI-ToF mass spectrum of **P6** was recorded which confirmed the proposed structure (see SI, Fig. S66).

Next, the scope of the polymerization of the tubular helix forming aromatic amino acid monomer (**M4**) was also investigated in DMAc. Thus, **M4** was polymerized with aniline (M/I = 30) and **PHOS3** in DMAc at rt under slow addition condition. Interestingly, SEC analysis of the obtained polymer (**P10**) shows an excellent control over molecular weight and appeared to be a good fit with the molar mass of the polymer (**P8**) obtained in chloroform at a similar monomer to initiator ratio. This confirmed the polymerization efficacy of **M4** with **PHOS3** in DMAc (see Table 3). Next, we investigated the polymerization of **M4** with a functional initiator *N*-Boc-p-phenylenediamine (**I3**) and **PHOS3**. SEC analysis of the crude polymer (**P11**) and ^{1}H NMR analysis of the purified polymer confirmed the excellent control over molecular weight and the presence of desired end group (see SI, Fig. S41 and S56).

After that, two further polymerizations of **M4** were performed with aniline and **PHOS3** by adjusting the monomer to the initiator ratio to 80 and 120. Although both polymers (**P12**, and **P13**) appeared to form a clear solution in DMF, SEC analyses of both polymers were unsuccessful. We believe the obtained high molecular weight helical polymers could not be eluted in SEC due to the formation of aggregates. This was confirmed later by small angle X-ray scattering (SAXS) and dynamic light scattering (DLS). A recent report by the Zhong et al. showed for the first time that well-defined oligomeric helices of this type can form double helical structures.[56] Such double helical structure formations might be responsible for the observed aggregation of oligomeric and polymeric helices (vide supra).

Nonetheless, the number average molecular weight of the obtained polymer **P12** and **P13** was determined by ^{1}H NMR

spectroscopy by exploiting the significant difference between the end group and backbone ^{1}H-NMR signals and appeared to be a good match with the target values (Table 3 and SI Fig. S42-S45). We assume that the polymers **P12** and **P13** adopt a similar helical geometry as those previously reported by the Gong group. There, single crystal x-ray structures could be obtained for well-defined oligomeric helices which showed that 6.6 monomer units formed one helical turn with a pitch of 3.4 Å.[26] This would correspond to a helix length of ca. 4.1 nm for **P12** and 6.2 nm for **P13**.

Table 3. Number average molecular weights (M_n) and polydispersity indexes ($Đ = M_w/M_n$) of the polymers synthesized with monomer **M4**

Polymer	M/I	M_n-theo [kDa][a]	M_n-SEC [kDa][b]	M_n-NMR [kDa][c]	Đ[b]
P6	10	3.7	3	4.1	1.08
P7	20	7.5	6.4	10.1	1.09
P8	30	11.2	9.7	16.1	1.18
P9	40	15	13.9	21	1.24
P10	30	11.2	10.3	13.5	1.34
P11	10	3.7	3.1	5.3	1.09
P12	80	30	-	37.5	-
P13	120	45	-	49.8	-

a Theoretical Molecular weight.

b Molecular weight and dispersity determined by SEC in DMF.

c Molecular weight determined by ^{1}H NMR spectroscopy.

Next, to confirm the superstructure formation of the obtained polymer from monomer **M4**, polymer **P13** was analyzed by atomic force microscopy (AFM). Several micrometer-long sheet-like superstructures and a nano-scale rod-like structure were detected in AFM (see Figure 3, SI). We assume that due to the presence of hydrophobic ethylhexyl side chains, the individual rod-like tubular helices aggregate to form a higher-order sheet-like structure. Scanning electron microscopy (SEM) of **P13** also revealed a similar sheet-like higher-order structure (see Figure 3, SI).

Furthermore, the solution structure of **P13** was also analyzed by small angle X-ray scattering (SAXS) in THF and DMF (Figure 4). The SAXS data in THF show a local stiffness region, following a q^{-1} decay of the scattering data between around 1 and 3 nm^{-1}. This region was absent for **P13** in DMF. It indicates structural motives with 1-2 nanometer dimensions, most likely from the cross-section scattering of the helix in THF, most likely due to the linear self-assembly of this polymer. This nanoscale structure was absent in DMF. Furthermore, larger supramolecular structures were observed in THF and DMF. The dimensions of these structures exceed the resolution limit of our SAXS set-up with $\frac{2\pi}{q_{min}} \sim 100\ nm$. These supramolecular structures may be polymer fibrils with the low-q power-law scattering following $q^{-2.3}$ in THF and $q^{-1.8}$ in DMF, representing theta solvent and good solvent conditions, respectively. A solvent like DMF is well known to effectively interrupt the inter-chain aggregation of aromatic oligoamide foldamers such as macrocycles and helices.[53,54]

We believe that, similarly, in the case of **P13** in DMF the supramolecular aggregation of the helices is at least partially disrupted.

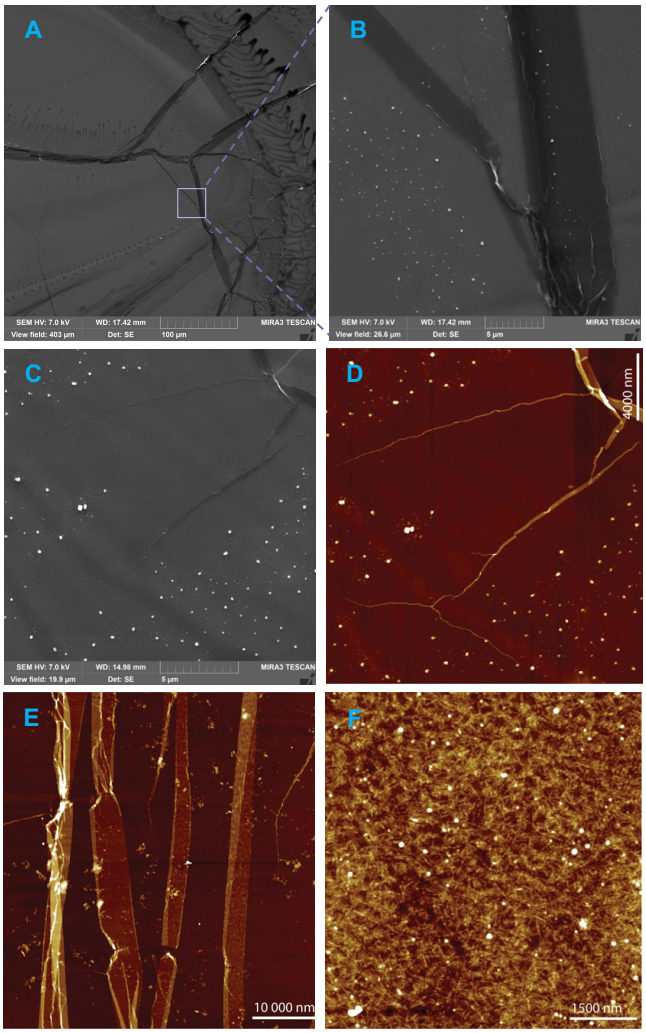

Figure 3. SEM and AFM analyses of the helical polymer **P13** with **PHOS3**.(A and B) SEM image of drop casted **P13** polymer (A) and zoom in of one spot (B). SEM (C) and AFM (D) of drop casted **P13** at the same position. (E) Sheet-like structure of drop casted **P13** was observed in AFM. (F) High-resolution AFM image of **P13** indicates the presence of unassembled/secondary building blocks for sheet-like superstructure formation.

Depolarized dynamic light scattering depends solely on particle anisotropy, with spherical particles yielding little to no depolarized scattering intensity.[57] A comparison of the intensity (count rate) of polarized (VV) against depolarized (VH) scattering can be used to gain insights into the degree of anisotropy of a sample (Figure 5). For the assemblies of **P13** in either THF or chloroform, the drop in intensity from VV to VH is around 1 order of magnitude, whereas for a spherical control (100 nm latex beads), the drop is much more pronounced, ca. 3 orders of magnitude.

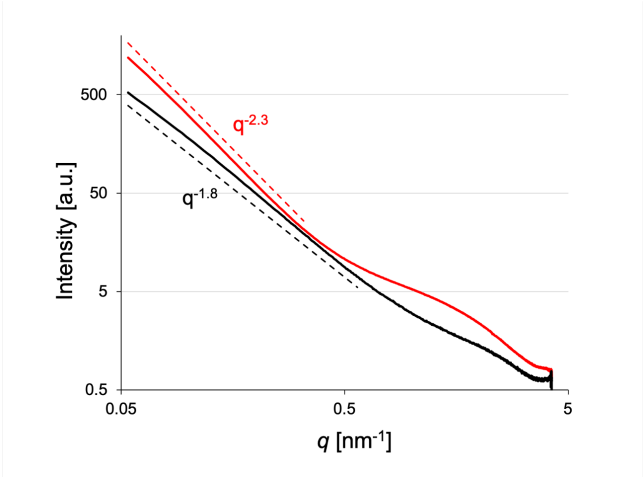

Figure 4. SAXS analyses of polymer **P13** in THF (red curve) and DMF (black curve). The calculated power-law curves are presented as dashed lines in the corresponding SAXS regions. A local structured region can be observed for **P13** in THF between 1 and 3 nm^{-1}, which may arise from the scattering of the cross-section of the helix together with local stiffness.

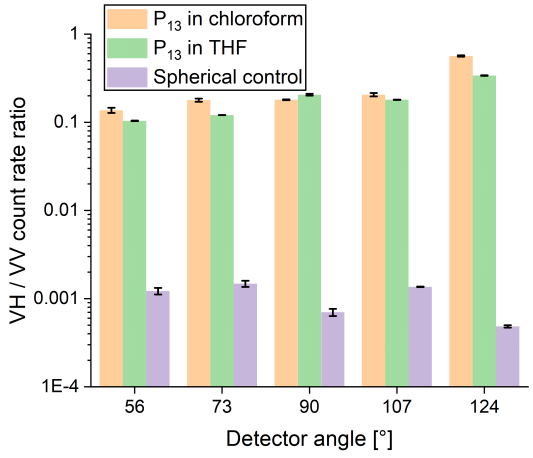

Figure 5. (De)polarized Dynamic Light Scattering analysis of polymer **P13**. Ratio between angular scattering intensities in depolarized (VH) and polarized (VV) mode for **P13** in THF and chloroform as well as comparison with spherical particles (latex beads). The drop in intensity from VV to VH is much more intense for spherical control particles as compared to **P13**, which is a result of optical anisotropy of the polymer assemblies.

This difference could be explained by the optical anisotropy of **P13** assemblies, which is an indication that **P13** likely forms elongated supramolecular structures in both chloroform and THF. The hydrodynamic radii (R_h) obtained for **P13** from the VV autocorrelation curves (Figure S67) are within the 68-80 nm range for both THF and chloroform, evidence of the nanoscale of the supramolecular assemblies, although real dimensions of elongated structures can considerably differ from their R_h.

The helical structure of the polymer **P13** was supported through chiral induction with L-arginine via the domino effect.[58] The racemic foldamers have previously been chirally enriched via chiral molecule recognition.[59,60,61] The foldamer obtained from monomers like **M4** are well known to recognize guanine.[62] Hence, **P13** was treated with L-arginine in DMF at 80 °C, followed by dilution with chloroform. Then, the solution was equilibrated for 12 hours at rt, and the CD spectrum was recorded. Interestingly, an intense CD signal was observed and further supported the helical nature of the polymer **P13** (see SI, Fig. S59).

Conclusions

In conclusion, we have developed a new phosphorous-based reagent (**PHOS3**) that selectively activates carboxylic acids in H-bond-breaking solvents like DMAc and NMP. Moreover, the newly designed reagent shows inertness toward aromatic primary and secondary aromatic amines even at elevated temperatures. The fast activation of carboxylic acid by **PHOS3** allows the living polymerization of non-self-deactivating aromatic amino acid monomer and oligomer under slow addition polymerization conditions. Therefore, it provided a new platform to synthesize living poly aromatic amides in H-bond-breaking solvents for the first time. Furthermore, narrow dispersed chiral helical diblock copolymers were also synthesized in DMAc with **PHOS3**. Aromatic helical foldamers are known to mimic biological functions; therefore, they are heavily investigated. Here, we have synthesized one of such tubular helices forming monomer and polymerized it with **PHOS3** in a living chain-growth manner under slow addition condition. The improved chemoselectivity and the thermal stability of **PHOS3** also allow the synthesis of the highest molecular weight tubular helices so far in a living manner in one step. The AFM, SEM, and SAXS analyses of these polymers support the helical nature of the polymer along with sheet-like tertiary structure formations. Overall, this demonstrates the huge potential of the newly developed **PHOS3** reagent and the polymerization method for aromatic foldamer and aramid-based supramolecular architectures design.

ASSOCIATED CONTENT

Supporting Information

The Supporting Information includes experimental procedures, NMR spectra, SEC elugrams, CD-spectra, SEM, AFM and TEM images, HRMS and MALDI-ToF mass spectra and polarized dynamic light scattering autocorrelation curves. The Supporting Information is available free of charge on the ACS Publications website.

AUTHOR INFORMATION

Corresponding Author

* Andreas Kilbinger. andreas.kilbinger@unifr.ch

Author Contributions

S.P. and A.F.M.K. designed the experiments. S.P. synthesized the phosphorous reagent, conducted all polymerizations and most polymer and molecular analyses. S. F. conducted several polymer analyses. L. H, R. V. M. F. and S. S conducted SAXS measurements. All authors reviewed the manuscript.

ACKNOWLEDGMENT

A. F. M. K, S. P, L. H, R. V. M. F., S. F. and S. S. thanks Swiss National Science Foundation, National Center of Competence in Research (NCCR Bio-inspired Materials) and the Fribourg Center for Nanomaterials (FriMat) for support.

REFERENCES

[1] Kwolek, S.L.; Morgan, P.W.; Schaefgen, J.R.; and Gulrich, L.W. Synthesis, Anisotropic Solutions, and Fibers of Poly(1,4-benzamide). *Macromolecules* **1977**, *10*, 1390–1396.

[2] Takahashi, Y.; Ozaki, Y.; Takase, M.; and Krigbaum, W.R. Crystal structure of poly(p-benzamide). *J. Polym. Sci. Part B Polym. Phys.* **1993**, *31*, 1135–1143.

[3] Schulze, M.; Michen, B.; Fink, A.; and Kilbinger, A.F.M. Bis-TEGylated Poly(p-benzamide)s: Combining Organosolubility with Shape Persistence. *Macromolecules* **2013**, *46*, 5520–5530.

[4] Yang, H. H. Aromatic High-Strength Fibers; John Wiley & Sons, Inc.: New York, 1989.

[5] Kwolek, S. L.; Morgan, P. W.; Sorenson, W. R. Process of Making Wholly Aromatic Polyamides. U.S. Patent 3063966, 1962.

[6] Zhang, D.-W.; Zhao, X.; Hou, J.-L.; and Li, Z.-T. Aromatic Amide Foldamers: Structures, Properties, and Functions. *Chem. Rev.* **2012**, *112*, 5271–5316.

[7] Hecht, S.; Huc, I. Foldamers: Structure, Properties and Applications; Wiley–VCH: Weinheim, Germany, 2007.

[8] Hill, D.J.; Mio, M.J.; Prince, R.B.; Hughes, T.S.; and Moore, J.S. A Field Guide to Foldamers. *Chem. Rev.* **2001**, *101*, 3893–4012.

[9] Li, Z.-T.; Hou, J.-L.; Li, C.; and Yi, H.-P. Shape-Persistent Aromatic Amide Oligomers: New Tools for Supramolecular Chemistry. *Chem. – An Asian J.* **2006**, *1*, 766–778.

[10] Gong, B. Molecular Duplexes with Encoded Sequences and Stabilities. *Acc. Chem. Res.* **2012**, *45*, 2077–2087.

[11] Bohle, A.; Brunklaus, G.; Hansen, M.R.; Schleuss, T.W.; Kilbinger, A.F.M.; Seltmann, J.; and Spiess, H.W. Hydrogen-Bonded Aggregates of Oligoaramide–Poly(ethylene glycol) Block Copolymers. *Macromolecules* **2010**, *43*, 4978–4985.

[12] Seyler, H.; and Kilbinger, A.F.M. Hairy Aramide Rod–Coil Copolymers. *Macromolecules* **2010**, *43*, 5659–5664.

[13] Badoux, M.; Drechsler, S.; Pal, S.; and Kilbinger, A.F.M. Facile Synthesis of a High Molecular Weight Amphiphilic Aramid-ROMP Block Copolymer. *Macromolecules* **2017**,*50*, 9307–9314.

[14] Schleuss, T.W.; Abbel, R.; Gross, M.; Schollmeyer, D.; Frey, H.; Maskos, M.; Berger, R.; and Kilbinger, A.F.M. Hockey-Puck Micelles from Oligo(p-benzamide)-b-PEG Rod–Coil Block Copolymers. *Angew. Chemie Int. Ed.* **2006**, *45*, 2969–2975.

[15] van Gorp, J.J.; Vekemans, J.A.J.M.; and Meijer, E.W. C3-Symmetrical Supramolecular Architectures: Fibers and Organic Gels from Discotic Trisamides and Trisureas. *J. Am. Chem. Soc.* **2002**, *124*, 14759–14769.

[16] Wilson, A.J.; van Gestel, J.; Sijbesma, R.P.; and Meijer, E.W. Amplification of chirality in benzene tricarboxamide helical supramolecular polymers. *Chem. Commun.* **2006**, 4404–4406.

[17] Wilson, A.J.; Masuda, M.; Sijbesma, R.P.; and Meijer, E.W. Chiral Amplification in the Transcription of Supramolecular Helicity into a Polymer Backbone. *Angew. Chemie Int. Ed.* **2005**, *44*, 2275–2279.

[18] Christoff-Tempesta, T.; Cho, Y.; Kim, D.-Y.; Geri, M.; Lamour, G.; Lew, A.J.; Zuo, X.; Lindemann, W.R.; and Ortony, J.H. Self-assembly of aramid amphiphiles into ultra-stable nanoribbons and aligned nanoribbon threads. *Nat. Nanotechnol.* **2021**, *16*, 447–454.

[19] Yang, M.; Cao, K.; Sui, L.; Qi, Y.; Zhu, J.; Waas, A.; Arruda, E.M.; Kieffer, J.; Thouless, M.D.; and Kotov, N.A. Dispersions of Aramid Nanofibers: A New Nanoscale Building Block. *ACS Nano* **2011**, *5*, 6945–6954.

[20] Ziach, K.; Chollet, C.; Parissi, V.; Prabhakaran, P.; Marchivie, M.; Corvaglia, V.; Bose, P.P.; Laxmi-Reddy, K.; Godde, F.; Schmitter, J.-M.; et al. Single helically folded aromatic oligoamides that mimic the charge surface of double-stranded B-DNA. *Nat. Chem.* **2018**, *10*, 511–518.

[21] De, S.; Chi, B.; Granier, T.; Qi, T.; Maurizot, V.; and Huc, I. Designing cooperatively folded abiotic uni- and multimolecular helix bundles. *Nat. Chem.* **2018**, *10*, 51–57.

[22] Gan, Q.; Wang, X.; Kauffmann, B.; Rosu, F.; Ferrand, Y.; and Huc, I. Translation of rod-like template sequences into homochiral assemblies of stacked helical oligomers. *Nat. Nanotechnol.* **2017**, *12*, 447–452.

[23] Gong, B.; Zeng, H.; Zhu, J.; Yua, L.; Han, Y.; Cheng, S.; Furukawa, M.; Parra, R.D.; Kovalevsky, A.Y.; Mills, J.L.; et al. Creating nanocavities of tunable sizes: Hollow helices. *Proc. Natl. Acad. Sci.* **2002**, *99*, 11583–11588.

[24] Yuan, L.; Zeng, H.; Yamato, K.; Sanford, A.R.; Feng, W.; Atreya, H.S.; Sukumaran, D.K.; Szyperski, T.; and Gong, B. Helical Aromatic Oligoamides: Reliable, Readily Predictable Folding from the Combination of Rigidified Structural Motifs. *J. Am. Chem. Soc.* **2004**, *126*, 16528–16537.

[25] Koehler, V.; Roy, A.; Huc, I.; and Ferrand, Y. Foldaxanes: Rotaxane-like Architectures from Foldamers. *Acc. Chem. Res.* **2022**, *55*, 1074–1085.

[26] Zhong, Y.; Kauffmann, B.; Xu, W.; Lu, Z.-L.; Ferrand, Y.; Huc, I.; Zeng, X.C.; Liu, R.; and Gong, B. Multiturn Hollow Helices: Synthesis and Folding of Long Aromatic Oligoamides. *Org. Lett.* **2020**, *22*, 6938–6942.

[27] Roy, A.; Joshi, H.; Ye, R.; Shen, J.; Chen, F.; Aksimentiev, A.; and Zeng, H. Polyhydrazide-Based Organic Nanotubes as Efficient and Selective Artificial Iodide Channels. *Angew. Chemie Int. Ed.* **2020**, *59*, 4806–4813.

[28] Gong, B. Hollow Crescents, Helices, and Macrocycles from Enforced Folding and Folding-Assisted Macrocyclization. *Acc. Chem. Res.* **2008**, *41*, 1376–1386.

[29] Huc, I. Aromatic Oligoamide Foldamers. European *J. Org. Chem.* **2004**, 17–29.

[30] Schulze, M.; and Kilbinger, A.F.M. Toward large tubular helices based on the polymerization of tri(benzamide)s. *J. Polym. Sci. Part A Polym. Chem.* **2016**, *54*, 1731–1741.

[31] Pal, S.; Nguyen, D.P.T.; Molliet, A.; Alizadeh, M.; Crochet, A.; Ortuso, R.D.; Petri-Fink, A.; and Kilbinger, A.F.M. A versatile living polymerization method for aromatic amides. *Nat. Chem.* **2021**, *13*, 705–713.

[32] Ferguson, J.S.; Yamato, K.; Liu, R.; He, L.; Zeng, X.C.; and Gong, B. One-Pot Formation of Large Macrocycles with Modifiable Peripheries and Internal Cavities. *Angew. Chemie Int. Ed.* **2009**, *48*, 3150–3154.

[33] Shen, J.; Fan, J.; Ye, R.; Li, N.; Mu, Y.; and Zeng, H. Polypyridine-Based Helical Amide Foldamer Channels: Rapid Transport of Water and Protons with High Ion Rejection. *Angew. Chemie Int. Ed.* **2020**, *59*, 13328–13334.

[34] Chandramouli, N.; Ferrand, Y.; Lautrette, G.; Kauffmann, B.; Mackereth, C.D.; Laguerre, M.; Dubreuil, D.; and Huc, I. Iterative design of a helically folded aromatic oligoamide sequence for the selective encapsulation of fructose. *Nat. Chem.* **2015**, *7*, 334–341.

[35] Ferrand, Y.; and Huc, I. Designing Helical Molecular Capsules Based on Folded Aromatic Amide Oligomers. *Acc. Chem. Res.* **2018**, *51*, 970–977.

[36] Gan, Q.; Ferrand, Y.; Bao, C.; Kauffmann, B.; Grélard, A.; Jiang, H.; and Huc, I. Helix-Rod Host-Guest Complexes with Shuttling Rates Much Faster than Disassembly. *Science* **2011**, *331*, 1172–1175.
[37] Zhou, X.; Liu, G.; Yamato, K.; Shen, Y.; Cheng, R.; Wei, X.; Bai, W.; Gao, Y.; Li, H.; Liu, Y.; et al. Self-assembling sub-nanometer pores with unusual mass-transport properties. *Nat. Commun.* **2012**, *3*, 949.
[38] Gong, B.; and Shao, Z. Self-Assembling Organic Nanotubes with Precisely Defined, Sub-nanometer Pores: Formation and Mass Transport Characteristics. *Acc. Chem. Res.* **2013**, *46*, 2856–2866.
[39] Shen, Y.; Fei, F.; Zhong, Y.; Fan, C.; Sun, J.; Hu, J.; Gong, B.; Czajkowsky, D.M.; and Shao, Z. Controlling Water Flow through a Synthetic Nanopore with Permeable Cations. *ACS Cent. Sci.* **2021**, *7*, 2092–2098.
[40] Shen, J.; Ye, R.; Romanies, A.; Roy, A.; Chen, F.; Ren, C.; Liu, Z.; and Zeng, H. Aquafoldmer-Based Aquaporin-like Synthetic Water Channel. *J. Am. Chem. Soc.* **2020**, *142*, 10050–10058.
[41] Yamazaki, N.; Higashi, F. Studies on reactions of N-phosphonium Salts of Pyridines. VIII. Preparation of Polyamides by Means of Diphenyl Phosphite in Pyridine. *J. Polym. Sci.; Polym. Lett. Ed.* **1974**, *12*, 185–191.
[42] Wu, G.-C.; Tanaka, H.; Sanui, K.; Ogata, N. Synthesis of Poly (p- benzamide) with Triphenylphosphine and Hexachloroethane Reagents Reaction Conditions. *Polym. J.* **1982**, *14*, 571–574.
[43] Carothers, W. H. Polymers and polyfunctionality. *Trans. Faraday Soc.* **1936**, *32*, 39–49.
[44] Yokozawa, T.; and Yokoyama, A. Chain-Growth Condensation Polymerization for the Synthesis of Well-Defined Condensation Polymers and π-Conjugated Polymers. *Chem. Rev.* **2009**, *109*, 5595–5619.
[45] Yokozawa, T.; and Ohta, Y. Transformation of step-Growth polymerization into living chain-Growth polymerization. *Chem. Rev.* **2016**, *116*, 1950–1958.
[46] Mikami, K.; and Yokozawa, T. Helical folding of poly(naphthalenecarboxamide) in apolar solvent. *J. Polym. Sci. Part A Polym. Chem.* **2013**, *51*, 739–742.
[47] Yokozawa, T.; and Ohta, Y. Scope of controlled synthesis via chain-growth condensation polymerization: from aromatic polyamides to π-conjugated polymers. *Chem. Commun.* **2013**, *49*, 8281–8310.
[48] Yokozawa, T.; Asai, T.; Sugi, R.; Ishigooka, S.; and Hiraoka, S. Chain-Growth Polycondensation for Nonbiological Polyamides of Defined Architecture. *J. Am. Chem. Soc.* **2000**, *122*, 8313–8314.
[49] Sugi, R.; Yokoyama, A.; Furuyama, T.; Uchiyama, M.; and Yokozawa, T. Inductive Effect-Assisted Chain-Growth Polycondensation. Synthetic Development from para- to meta-Substituted Aromatic Polyamides with Low Polydispersities. *J. Am. Chem. Soc.* **2005**, *127*, 10172–10173.
[50] Ohishi, T.; Sugi, R.; Yokoyama, A.; and Yokozawa, T. A variety of poly(m-benzamide)s with low polydispersities from inductive effect-assisted chain-growth polycondensation. *J. Polym. Sci. Part A Polym. Chem.* **2006**, *44*, 4990–5003.
[51] Badoux, M.; and Kilbinger, A.F.M. Synthesis of High Molecular Weight Poly(p-benzamide)s. *Macromolecules* **2017**, *50*, 4188–4197.
[52] Sawamoto, M.; and Kennedy, J.P. Quasiliving Carbocationic Polymerization. VIII. Quasiliving Polymerization of Methyl Vinyl Ether and Its Blocking from Quasiliving Poly(isobutyl Vinyl Ether) Dication. *J. Macromol. Sci. Part A - Chem.* **1982**, *18*, 1301–1313.
[53] Sobiech, T.A.; Zhong, Y.; Gong, B. Cavity-containing aromatic oligoamide foldamers and macrocycles: progress and future perspectives. *Org. Biomol. Chem.*, **2022,** 6962-6978.
[54] Yang, Y.; Feng, W.; Hu, J.; Zou, S.; Gao, R.; Yamato, K.; Kline, M.; Cai, Z.; Gao, Y.; Wang, Y.; Li, Y.; Yang, Y.; Yuan, L.; Zeng, X. C.; Gong, B. Strong Aggregation and Directional Assembly of Aromatic Oligoamide Macrocycles. *J. Am. Chem. Soc.* **2011**, *133*, 18590-18593.
[55] Urushibara, K.; Masu, H.; Mori, H.; Azumaya, I.; Hirano, T.; Kagechika, H.; and Tanatani, A. Synthesis and Conformational Analysis of Alternately N-Alkylated Aromatic Amide Oligomers. *J. Org. Chem.* **2018**, *83*, 14338–14349.
[56] Zhong, Y.; Sobiech, T.A.; Kauffmann, B.; Song, B.; Li, X.; Ferrand, Y.; Huc, I.; Gong, B. High-affinity single and double helical psudofoldaxanes with cationic guests. *Chem. Sci.* **2023**, *14*, 4759-4768.
[57] Zero, K.; Pecora, R. in Dynamic Light Scattering: Applications of Photon Correlation Spectroscopy; Pecora, R.; Ed.; Plenum: New York, 1985; p 59.
[58] Zhang, D.-W.; Wang, H.; and Li, Z.-T. Polymeric Tubular Aromatic Amide Helices. Macromol. Rapid Commun. 2017, 38, 1700179.
[59] Zhang, P.; Zhang, L.; Wang, Z.-K.; Zhang, Y.-C.; Guo, R.; Wang, H.; Zhang, D.-W.; and Li, Z.-T. Guest-Induced Arylamide Polymer Helicity: Twist-Sense Bias and Solvent-Dependent Helicity Inversion. *Chem. – An Asian J.* **2016**, *11*, 1725–1730.
[60] Lautrette, G.; Wicher, B.; Kauffmann, B.; Ferrand, Y.; and Huc, I. Iterative Evolution of an Abiotic Foldamer Sequence for the Recognition of Guest Molecules with Atomic Precision. *J. Am. Chem. Soc.* **2016**, *138*, 10314–10322.
[61] Dolain, C.; Jiang, H.; Léger, J.-M.; Guionneau, P.; and Huc, I. Chiral Induction in Quinoline-Derived Oligoamide Foldamers: Assignment of Helical Handedness and Role of Steric Effects. *J. Am. Chem. Soc.* **2005**, *127*, 12943–12951.
[62] Sanford, A.R.; Yuan, L.; Feng, W.; Yamato, K.; Flowers, R.A.; and Gong, B. Cyclic aromatic oligoamides as highly selective receptors for the guanidinium ion. *Chem. Commun.* **2005**, 4720–4722.

graphical abstract